Application of Radon Fan Transform in Systems of Correlation Analysis and Localization of Acoustic Noises

Oleksandr Ponomarenko [1], Mykola Vinohradov [2], Svitlana Kovtun [1], Anna Krymska [1]

[1] *General energy Institute of NAS of Ukraine, Antonovich str., 172, Kyiv, 03150, Ukraine*
[2] *National Aviation University, Liubomyra Huzara ave., 1, Kyiv, 03058, Ukraine*

Abstract

Locating fluid leaks from pressurized pipelines is a serious problem, especially for hidden pipelines. In this case, it is necessary to apply remote sensing methods with combined (linear and angular) scanning of acoustic noise sensors. There are two main instrumental methods for determining leaks in pipelines, namely, tomographic acoustic method and correlation noise-meter one. This paper represents the results of development of the method of detection of acoustic noise signals generated at the expiration of a fluid through a defect of a pipeline. The fundamental difference of this method is to refine the model of useful and interfering signals, such as data loss and noise. The results of theoretical analysis of the detection method and the coordinate measuring acoustic source are presented. Proposed method can be the theoretical basis for creation a computerized system with multi-site tomographic detection on incomplete and noisy data.

Keywords

Radon fan transform, tomographic signal processing, multi-site tomographic detection on incomplete and noisy data

1. Introduction

The energy security of the country depends, first of all, on the reliability and technical condition of energy facilities, and when providing consumers with thermal energy, it depends not least on the condition of pipelines of heat networks. In recent decades, the method of acoustic contact leak detection has been widely used for operational control of pipelines tightness [1–7]. Detection of leaks by this method is based, as a rule, on the analysis of correlation-spectral characteristics of acoustic noise signals generated by liquid leakage through a defect in the control object [8-10]. However, in the case of underground laying of heat pipes, the use of contact methods can cause certain difficulties.

Traditional leak detection devices and systems are built according to the correlation scheme, which is good for pipelines running along the surface. However, the measurement accuracy for buried (underground or underwater) pipelines is poor and deteriorates rapidly with increasing pipeline depth. In these cases, it is necessary to apply remote sensing methods with a combined (linear and/or circular) arrangement of sensors [11]. Modern remote sensing of hidden pipelines is based on high-precision multi-position (multi-sensor) systems with tomographic signal processing. Any sensor from the set $S_1, S_2, \dots, S_N$ makes primary signal processing: noise filtration, amplification and preparation signal to transmission through telecommunication line. Then the information from the set of sensors is transferred to the system of joint signal processing. Control system (not shown) provides time matching of scanning and/or shift of sensors for observation the same viewpoint.

Proceedings ITTAP'2023: 3rd International Workshop on Information Technologies: Theoretical and Applied Problems, November 22–24, 2023, Ternopil, Ukraine, Opole, Poland
EMAIL: ponomarenkos_200@ukr.net (O.P.); mykola.vinohradov@npp.nau.edu.ua (M.V.); sveta_kovtun@ukr.net (S.K.); dep4_ize@ukr.net (A.K.)
ORCID: 0000-0002-6538-0468 (O.P.); 0000-0003-3614-042X (M.V.); 0000-0002-6596-3460 (S.K.); 0000-0001-6410-9476 (A.K.)

It’s necessary to get coordinates of source of acoustic noises after joint processing signals from N sensors.

Theoretically, it’s necessary to scan in spatial angle sector of 360 or, as minimum, 180 degrees for obtaining full image of source of acoustic signal. Such problem actually cannot be dissolved; so, obtaining detail image is impossible. When reconstructing images of point objects, tomography methods are used, in particular, the method of filtered back projections based on convolution [12, 13].

Theoretically, this problem belongs to the class of inverse problems of mathematical physics [14]. When receiving a certain set of signals from sensors located around an object in a limited angular sector, we obtain an incorrect mathematical problem [14].

Article [15] is devoted to aspects of applied problems of tomography, in particular, to the method of empirical elimination of incorrectness by introducing ρ-filtering. The authors substantiate this decision by the fact that low spatial frequencies of the Fourier image are determined in a larger number of points of the spectral plane, and high frequencies in a smaller number. Moreover, the density of specifying the spectral components decreases according to the law 1/ρ. Therefore, to restore the function before performing the two-dimensional inverse Fourier transform, it is necessary to first perform the convolution of the spatial spectrum with the ρ -function. This complex approach can be replaced by a simple and obvious transition from Cartesian (for the Fourier transform) to polar (for the Radon transform) coordinates with the Jacobian of the transformation |ρ|.

The work [16] also considers the practical aspects of the computer implementation of the Radon transform. The authors argue that the practical implementation of the discrete Radon transform is possible with the replacement of the conventional Radon transform with the Fast Fourier Transform (FFT). But the irregularity of samples with a circular or sector FFT at different distances leads to uncontrolled degradation of the angular resolution of the processing system.

The article [17] shows that the FFT can be used to calculate various generalizations of the classical Radon transform (RT), for example, as a linear algebra problem, and reduce it to solving a linear system of equations with a block circulant matrix. The stability of solutions, the accuracy of interpolation, and the efficiency of data permutation depend on a good choice of the inversion method. The approach proposed in [17] does not guarantee the achievement of these characteristics in most cases.

Obviously, it’s impossible to arrange in space the set of sensors sufficient for image acquisition of object and provide system synchronisation and control. Reconstructive computer tomography can be applied in acoustic detection and measurement systems just for enhancing efficiency (probability of detection, spatial resolution and measurement precision of coordinates of sources of acoustic signals). So, the image reconstruction of spatial acoustic field is made by incomplete and noisy data.

The most informative data for determination of acoustic signals sources, particularly, flaws in pipelines under high pressure, are functions of partial coherence and spatial mutual correlation functions of acoustic fields. These functions have essential distinctions for situations of presence and absence of flaws. These functions have substantial distinctions for cases absences and presences of losses: in first case they do not have the expressed regions of the surges, and in the second such surges are observed. The function of coherent is, essentially, a mutual spectral density the received signals. With its help the width of spatial spectrum of signal is estimated, that allows doing the grounded choice of the band of analysis for the evaluation of function of mutual correlation. While reconstructing correlation function on their projections under various angles of signal receiving, we get an image of noise source in 3-dimensional space.

The method of restoring (reconstruction) of multidimensional functions is the problem of integral geometry [12]. Principal difference of considered problem is that source and sensor and object are not on the same line-of-site. Real measuring systems operate with the parts of surface XOY, $[x_{min} \le x \le x_{max}, y_{min} \le y \le y_{max}]$, and with arrangement sensors in limited sector fan Radon transform with specific Laplacian of transformation is applied.

The purpose of this work is research of features of Radon transform with application to the task of detection sources of acoustic signals by the methods of computed tomography.

2. Formulation of the problem

Let's consider the spatially coherent acoustic field in the environment. Let us direct the z-axis of the rectangular coordinate system vertically (across the wave guide), the y-axis along the wave propagation, and the x-axis across this direction (see fig. 1). In the vertical plane *YOZ*, the radiation from a point source arrives at the set of receiving points in the range of angles α, a.k.a. angle capture. This parameter characterizes the range of limits of receiving signals by sensors line, within which the field amplitude decreases with increasing distance from the point source inversely to the square of distance.

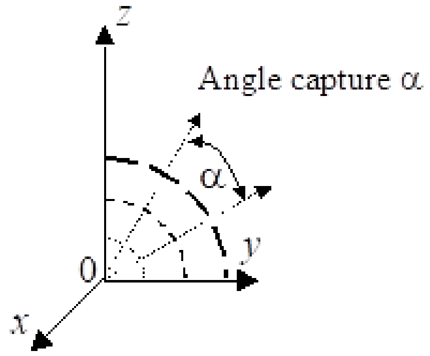

Figure 1: Ray propagation in angle capture

We'll consider quantitative communication between function of partial coherence and mutual power spectrum. If radiated signal exists on the interval $[-\overline{T,T}]$, then its Fourier transform $S(T,\nu)$ satisfies to Helmholtz equation

$$\nabla^2 S(T,\nu) + k^2 S(T,\nu) = 0, \qquad (1)$$

where ν is spatial frequency, $k = 2\pi/\lambda$ is wave number, λ is wavelength. Then formal decision of (1) with regards of N points of receiving of signal has form

$$S(r_i,T,\nu) = \sum_{i=1}^{N} k\, cos(\theta_i)\,(r_i,\nu) S(P_i,T,\nu)\; i = \overline{1,N}, \qquad (2)$$

where θ_i is the angle between line of sight of i^{th} sensor and vertical axis of coordinate system.

Using (2) we can calculate mutual power spectrum $I(P_1,P_2,\ldots,\nu)$, which actually represents function of multiple mutual coherence for the cases of presence and absence of flaws as sources of acoustic signals.

The problem of detection of acoustic signals, which appear due to outflows of liquid or fluid and are registered by sensor system, can be dissolved in the way of joint processing of acoustic noisy fields. If we receive some set of signals from sensors arranged around object in limited angular sector, Fourier transform changes on Radon transform [12].

When combined scanning sensors the problem of estimating the spectral and correlation characteristics of received noise signals is complicated: instead of the discrete Fourier transform is necessary to apply Chart Fan discrete Radon transform [12]. In this case the spatial spectrum of the field scattered by the noise source is a set of spatial frequencies, which are defined by the values of the corresponding angles.

For the problem considered adequately reflect the real situation of the additive mixture model acoustic noise source images and extraneous noise sources [12]:

$$\hat{G}(f_{xk}, f_{yk}) = G(f_{xk}, f_{yk}) + G_n(f_{xk}, f_{yk}),$$

where $G_n(f_{xk}, f_{yk}) = [V(f_{xk}, f_{yk})V^*(f_{xk}, f_{yk})]^{\frac{1}{2}} + N_0^{\frac{1}{2}}$; $V(f_{xk}, f_{yk})$ is the spatial spectrum of point and spatially distributed sources of interfering signals; N_{0i} – spectral density of the δ-correlated spatial noise.

Expanding the range of spatial frequencies in the spectrum is an advantage, since the thus reducing the influence of artefacts and decreases the overall level of the side lobes of the transfer function of the noise source. However, the information-processing algorithm becomes complicated due to continuous changes in the shape of two-dimensional spatial frequency spectrum. Almost unreal is an attempt to develop an algorithm of obtaining a tomographic image of the entire field of view of the extremely high requirements for search velocity, speed calculators and capacity data link capability. Therefore, it is advisable to develop a tomographic processing approach for an individual element of the spatial resolution for multi-site detector, coordinate measuring acoustic noise source.

3. The Modified Tomographic Processing Method by Shifted Segment of Spatial Spectrum

As it was shown in previous section, the set of aspect angles is limited, and spatial spectrum is shifted. Tomographic data processing is possible in both frequency and spatial domains. When processing in the frequency domain, strictly speaking, the cross section of the spatial spectrum at an angle $\theta_k = \varphi_k$ is a two-dimensional Fourier transform of the projection of the density of scattering angle φ_k or a one-dimensional Fourier transform in coordinates system $\{x_{\theta k}, y_{\theta k}\}$ along a coordinate $y_{\theta k}$ rotated relative to the Y -axis by the angle θ_k. However, if the real-scattered acoustic noise satisfies condition quasi-monochromatic approximation $\frac{\Delta f}{f_0 << 1}$, where Δf the width of the sound spectrum f_0 is average frequency of the noise signal we can approximately assume that the resultant received signal $G_k(x_k, y_k)$ from the direction θ_k is a function of the following form:

$$G_k(x_k, y_k) = \begin{cases} g_k(x_k, y_k) & if\ (x_k^2 + y_k^2)^2 = \frac{2}{\lambda}; \\ 0 & if\ (x_k^2 + y_k^2)^2 \neq \frac{2}{\lambda}, \end{cases} \quad (3)$$

where x_k, y_k are the projections of the spatial frequency spectrum at an angle θ_k to the axis f_x, f_y of the space-frequency plane. Then the general expression for the spatial spectrum image at multi-site receiving can be written as follows:

$$G_k(x_k, y_k) = G(f_{xk}, f_{yk}) =$$
$$= \sum_{k=1}^{N} g_k(x_k, y_k) exp\left\{-j\frac{4\pi}{\lambda \sec\left(\frac{\beta}{2}\right)}\left[y_k \cos\left(\frac{\varphi_0 + \varphi_k}{2}\right) - x_k \sin\left(\frac{\varphi_0 + \varphi_k}{2}\right)\right]\right\} =$$
$$= \sum_{k=1}^{N} g_k(x_k, y_k) exp\{-j2\pi(f_{xk}x_k + f_{yk}y_k)\}$$

where $f_{xk} = 2\sin\left(\frac{\varphi_0+\varphi_k}{2}\right) / \left(\lambda \sec\left(\frac{\beta_k}{2}\right)\right)$, $f_{yk} = -2\cos\left(\frac{\varphi_0+\varphi_k}{2}\right) / \left(\lambda \sec\left(\frac{\beta_k}{2}\right)\right)$ are components of the spatial frequency spectrum of acoustic noise, transformed with multi-site receiving. Transformation coefficient $\sec^{-1}\left(\frac{\beta_k}{2}\right)$ depends on the angle between the directions of rays of first and k^{th} receivers.

Thus, in the multi-position system with narrow band in the normal (frequency) sense acoustic signals we obtain a set of tomographic projections source at several spatial frequencies, which are defined by the values of the corresponding angles β_k.

When processing in the frequency domain in accordance with the expressions (3 - 4), we obtain a set of points in the polar raster, i.e., in coordinates θ_k. It is therefore logical to use the integral transformation in polar coordinates, i.e., Radon transform [12, 18]. Operation of calculus the intensities in polar coordinates are made by the method of back projection based on the convolution. Each set of projections using this method can be processed independently of the others, which considerably simplifies the construction of the processing algorithm.

Let the spatial spectrum $V(f_{xk}, f_{yk})$ of the source of interfering signals corresponding to stationary random field with the autocorrelation function $R_V(\Delta x_k, \Delta y_k)$:

$$R_V(\Delta x_k, \Delta y_k) = \Re_2^{-1}\{V(f_{xk}, f_{yk}), V^*(f_{xk}, f_{yk})\}. \quad (5)$$

Here $V^*(f_{xk}, f_{yk}) = V(-f_{xk}, -f_{yk})$; $\Re_2^{-1}\{\cdot,\cdot\}$ is a symbol of the two-dimensional inverse Radon transform.

Then the expression (5) for the projection-off scattered in k^{th} signal direction based on the availability of noise and interference is written as

$$g_i(x_k, y_k) = \sum_{i=1}^{L} u_l k_\sigma \sqrt{2\sigma_l}\delta(x_0 - x_l, y_0 - y_l) exp[-jk_\Delta(\beta_{il})(x_l\overline{x_k} + y_l\overline{y_k})] +$$
$$+ \sum_{m=1}^{M} V_m(x_k, y_k)\delta(x_0 - x_l, y_0 - y_l) + N_{0i} \tag{6}$$

The functions k_σ and k_δ are treated as a kernel of the transform (6) in the spatial coordinates.

Let's consider the sequence of processing steps according to the method of inverse projections [15]. A one-dimensional Fourier transform of the spatial spectrum $G(f_x, f_y)$ on a spatial frequency (for example f_x) has the form

$$g(x_k, f_{yk}) = \int_{-\infty}^{\infty} G(f_x, f_y)\, exp(-j2\pi f_{xk} x_k)\, df_x. \tag{7}$$

Performing Fourier transform on the other coordinate spatial frequency f_y, we get the image function

$$g(x_k, y_k) = \int_{-\infty}^{\infty} g(x_k, f_{yk})\, exp(-j2\pi f_{yk} y_k)\, df_y. \tag{8}$$

Let us come in (7 - 8) to polar coordinates in the field of spatial frequencies:

$$g(x_k, y_k) = \int_{-\pi}^{\pi} d\theta \int_{-\infty}^{\infty} G(\rho_k, \theta_k)|\rho|\, exp[-j2\pi\rho\, cos(\theta_k - \varphi_k)]\, d\rho, \tag{9}$$

where $|\rho|$ is the factor of transition to polar coordinates (Jacobian transformation).

Actually, the transition to polar coordinates in the expression (9) is a transition from the Fourier transform to the Radon transform.

To replace the direct convolution by fast convolution [19], we introduce the following notation:

$$\int_{-\infty}^{\infty} G(\rho_k, \theta_k)|\rho|\, exp[-j2\pi\rho r\, cos(\theta_k - \varphi_k)]\, d\rho = \Re[G(\rho_k, \theta_k)|\rho|].$$

$\Re[\cdot]$ is a symbol of Radon transform.

Because of the uneven arrangement of samples in the plane type algorithms (9) cannot be directly implemented, for example, using a fast Fourier transform processor (FFT). The inner integral of expression (9) should be submitted as an integral Fourier-Stieltjes. Then the expression (8) for all of the radiating section takes the following form:

$$g(x_k, y_k) = \int_{\theta_{min}}^{\theta_{max}} d\theta \int_{\rho_{min}}^{\rho_{max}} G(\rho, \theta)|\rho| exp[-j2\pi\rho r_k \cos(\theta_k - \varphi_k)] dP(\rho) +$$
$$+ \int_{\theta_{min}}^{\theta_{max}} d\theta \int_{\rho_{min}}^{\rho_{max}} G(\rho_n, \theta)|\rho_n| exp[-j2\pi\rho_n r_k \cos(\theta_k - \varphi_k)] dP(\rho_n) \tag{10}$$

and $P(\rho) = \{\rho_1, \rho_2, \dots, \rho_N\}$ are discrete samples of the function $|\rho|$ that in the method of inverse projection based on convolution kernel are treated as kernel of conversion (9) in the area of spatial frequencies [11]; $\rho_n = 2/\lambda_n$, $\lambda_{n,min} \le \lambda_n \le \lambda_{n,max}$.

However, receiver in k^{th} position with a bandwidth $\Delta f = f_{max} - f_{min} = \frac{c}{\lambda_{min}} - \frac{c}{\lambda_{max}}$ in the expression (10) the limits of integration in the second term ρ_{min}, ρ_{max} can be replaced by $\rho_{dm.min}, \rho_{dm,max}$, respectively:

$$\rho_{dm.min} = \frac{2}{\lambda_{max}} = \frac{2f_{min}}{c},\ \rho_{dm,max} = \frac{2}{\lambda_{min}} = \frac{2f_{max}}{c}.$$

Figure placing samples of the spatial spectrum of the useful signals (acoustic noise) and noise (noise of the receiver and the interfering source) is shown in Fig. 2.

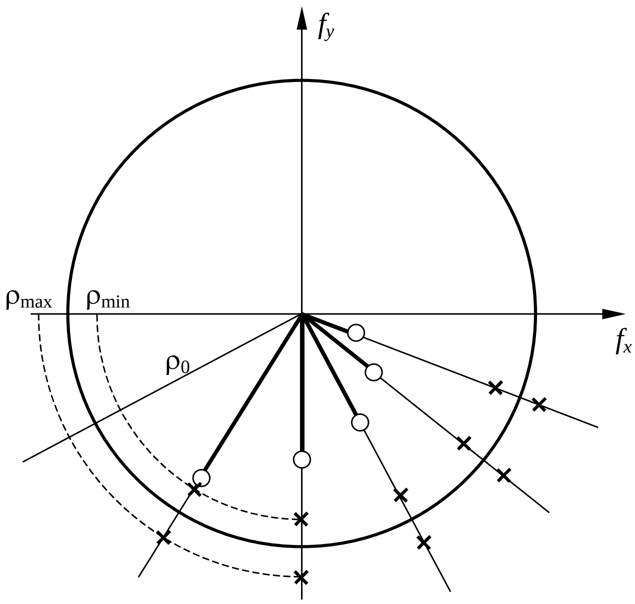

Figure 2: Diagram of placement of samples the spatial spectrum

On this spatial spectrum accurately restore function using the transformation (5 - 6), since the problem becomes non-correct. Incorrectness due to the presence of the second term on the right side of the expression (10). The weighting function or window function enhances the effect of the Radon transform in the high-frequency noise and interference, which in themselves are broadband. This leads to the loss of stability of the solution due to small variations of initial data. To build sustainable solutions to the equation (10) must be modified (regularize) window function:

$$k_c(\rho) = |\rho| k_p(\rho, \alpha), \tag{11}$$

where α is regularization parameter, typically selected based on the source data assignment errors. In this problem, α is chosen on energy and spectral characteristics of the noise considerations.

Essentially, regularizations in computer tomography tasks are smoothing weight function of two-dimensional ρ-filter.

Formally defined weighing function $|\rho|$ in finite region has high level of side lobes of transform, especially for fan Radon transform. So, we propose to smooth sharp edges of weighting function. It was established after comparative analysis of large number of various weighting functions that the most closed to optimal weighting function by the minimum of side lobes and acceptable dilatation of main lobes is the module of first derivative of Gaussian function:

$$\rho_w(x) = \left| \frac{d}{dx} [a \cdot exp(-bx^2)] \right| = ab \cdot |2x \cdot exp(-bx^2)|, \tag{12}$$

where a, b are constants of normalization. Choosing the values of constants a, b, you can optimize the ratio of the width of the space-frequency spectrum and the level of the side lobes.

As it's known, the Fourier transform of Gaussian function gives the spectral characteristic without side lobes. The derivative of Gaussian function represents linear conversion, so its Fourier transform must hasn't side lobes as well. Strictly speaking, the module of derivative of Gaussian function is non-linear conversion, which has the first order gap in zero. So, we can see one side lobe in the section of image, which actually is Radon transform of point object. However, the level of this lobe is rather small, smoothly and quickly falling, and due to small level and monotonous decreasing of side lobes the risk of appearance of false images (artefacts) resulting from random character of acoustic signal, is minimal.

Now we'll represent the results of synthesis of detector-meter grounding obtained data.

4. Synthesis detector-meter based on a modified Radon transform

Since the function is processed in a limited receiver bandwidth, it is a function of bounded variation. Therefore, the function $\hat{g}(r, \varphi)$ as a linear transformation $\hat{G}(\rho, \theta)$ is a function of bounded variation. If to apply such a function a regularisation with the exact values of the initial data ($G_n(\rho,\theta) = 0$), the regularised solution uniformly over (x, y) or what is the same, according to (r, φ) converges to the exact solution at $\alpha \to 0$. Therefore, in the future we will hold only a quantitative comparative analysis of errors due to regularization and the presence of interference.

Weighting windows are rotationally symmetric. The axis of symmetry coincides with the vertical axis of the system of spatial frequency coordinates. Weigh data only on the coordinate r. However, the processing of data in the segment, the limited range of angles $(\theta_{min}, \theta_{max})$, it is necessary to apply weighting to the coordinate θ as well.

When choosing a method of weighing the coordinate q is necessary to consider the following factors.

1. The data sets are very sparse.
2. The sequences of samples at θ are not equidistant.
3. Interfering signals (e.g., point sources of interference) may have very specific spatial characteristics (e.g., with an alternating spatial correlation coefficients).

When using a uniform weighting ($k(\theta) = 1$ if $\theta_{min} \leq \theta \leq \theta_{max}$, $k(\theta) = 0$ in other θ) achieved the highest resolution, but we have the Gibbs ripple. Their presence leads to additional artefacts in the reconstructed image. When using the weighted windows with recession towards the edges is deteriorating resolution of the system, but the main disadvantage of all of these windows is their monotonic dependence on the coordinates q. Because of this spatially correlated noise interfering sources not aligned with the source of interest will produce artefacts, which can mask the wanted signals (see Fig.3).

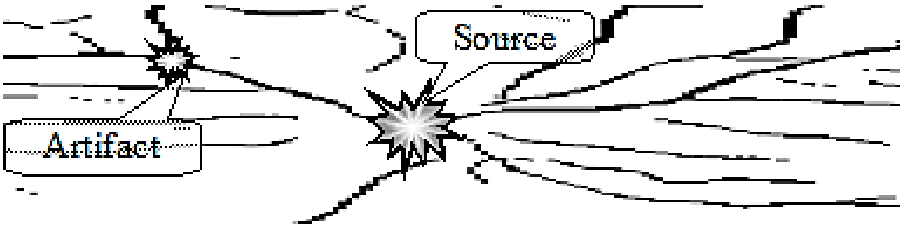

Figure 3: Spatial distribution of acoustic noise densities

To cancel such interference in the conditions of incomplete and non-equidistant sequences can be effectively used for evaluation of the spectrum maximum entropy method [19].

We write the expression for evaluating the image source of acoustic noise in the dense grid of spatial frequency coordinates θ_k (without weighting by θ):

$$\hat{g}(n_r, \varphi_k) = \sum_{m_\theta=-M}^{M} g_{\theta mp}(n_r, \varphi_k)\, exp\left[-j\frac{2\pi m_\theta n_r}{kN} cos(\theta_m - \varphi_k)\right].$$

The directions $\theta_m = \varphi_k$ the weights determined a priori space-correlation characteristics of acoustic noise. As in pipes under pressure as such characteristics may be used some average statistics on the results of experimental studies of acoustic noise arising from the rupture (fistula).

In all other directions the weights should be chosen by the criterion of maximum entropy with restrictions such as "correlation matching". If the sample in the direction of $\theta_k = \varphi_k$ the autocorrelation coefficients is assumed to be known and equal to $V_k(\varphi_k)$ the samples in another directions the autocorrelation coefficients $V_m(\theta_m)$ are determined by a priori characteristics of the internal noise of each of the N sensors. Let the spectral density of the noise k^{th} sensor is equal to N_k. Then the power spectral density $|g_{\theta mp}(n_r, \varphi_k)|^2$ of the sequence can be expressed in terms of certain factors like

$$|g_{\theta mp}(n_r, \varphi_k)|^2 = \begin{cases} \sum_{k=-N}^{N} V_k(\varphi_k) exp\left(-j2\pi\frac{kn_r}{N}\right) + \sum_{\substack{m=-M\\ m\neq k}}^{M} V_m(\theta_m) exp\left(-j2\pi\frac{mn_r}{M}\right) \quad M = kN \\ 0, \quad m > M, \;\; m < -M \end{cases} \tag{13}$$

Since the internal noise in the receiver spatial processing task are interpreted as spatial δ-correlated noise, and in the period gram $g(n_r, \varphi_k) = \{g_{\theta 1\rho}, g_{\theta 2\rho}, \dots, g_{\theta n\rho}\}$, $n_r = const$, the samples in the directions $\theta_m \neq \varphi_k$ should be δ-correlated random process. Under this condition, the resulting sequence (i.e., the sequence in which the signal samples are included with the autocorrelation coefficients $V_k(\varphi_k)$) will be a maximum entropy sequence.

Thus, the expression for evaluating the image (10) weighted by θ takes the following form:

$$\hat{g}(n_r,\varphi_k) = \sum_{k=-N}^{N} g_{\theta mp}(n_r,\varphi_k)\, exp\left[-j2\pi \frac{m_\theta n_r}{kN} cos(\theta_m - \varphi_k)\right] U(m_\theta)\, exp[-j2\pi\Phi(m)], \quad (14)$$

where

$$U(m_\theta) = \begin{cases} [V_k(\varphi_k)]^{\frac{1}{2}}, & \theta_m = \varphi_k; \\ [V_m(\theta_m)]^{\frac{1}{2}}, & \theta_m \neq \varphi_k; \end{cases} \quad (15)$$

$\xi_m = [V_m(\theta_m)]^{\frac{1}{2}}$ – Rayleigh random numbers from the distribution parameters define the characteristics of the internal noise of the sensor, which is calculated for the evaluation; $\Phi(m)$– uniformly distributed in the range of $\{-\pi,\pi\}$ random numbers. Both ξ_m and the $\Phi(m)$ numbers are independent.

If the inputs of the detecting-sensor measurement system, in addition to acoustic noise received noise signals with the same sign or an alternating spatial correlation coefficient, they respectively form (on the observation interval) on an alternating or monotonic sequence q. In both cases, sequences are spatially correlated. When multiplying this sequence to form a sequence of weighting coefficients (15) the resulting values are pseudo-random, and spatial correlation of interference signals is destroyed. There is a bleaching effect is spatially correlated noise, so, obviously, decreases the influence of artefacts caused by the regularity of the sequence structure of the interfering signals.

In accordance with the terms of spatial coordinates transform (9) $\theta_m = \theta_{nm} - \theta_{\text{sen}}$, wherein θ_{sen}– the angular direction of the receiving sensor.

We write the final realization of the algorithm tomographic processing system receiving sensor method regularized back projection based on the weighted convolution.

1. Sub algorithm of processing in i^{th} sensor.

   a) Sample preparation (projection) $g_i(x_k,y_k)$ in a coordinate system related to i^{th} sensor:

$$r_k = \left(x_k^2 + y_k^2\right)^{\frac{1}{2}}; \quad \phi_k = arctg\left(\frac{y_k}{x_k}\right).$$

   b) The calculation of the cross section of the spatial spectrum at an angle as the Radon transform projection angle φ_k:$G_i(\rho_k,\theta_k) = \Re_r\{g_i(r_k,\phi_k)\}$.

   c) Multiplication of the calculated images to weighting function.

   d) Calculation of the evaluation pseudo image of irradiated area in i^{th} sensor as an inverse Radon-Stieltjes transform of estimation of section of the spatial spectrum $\hat{G}_k(\rho_k,\theta_k) = G_i(\rho_k,\theta_k)U(\rho_k)$:

$$\hat{g}_i(r_k,\theta_k) = \Re_\rho^{-1}\{\hat{G}_i(r_k,\theta_k)\}. \quad (16)$$

2. Sub algorithm of joint data processing of all sensors of system

   a) Multiplication of the estimates (18) by the weighting functions $U_i(\theta_k)$ described by expression (15):

$$\hat{g}_w(r_k,\theta_k) = g_i(r_k,\theta_k)U_i(\theta_k).$$

   b) The calculation of the integral evaluation pseudo image analyses area as a set of inverse Radon transform for estimates $\hat{g}_w(r_k,\theta_k)$ for all discrete values θ_k for different values r_k: $g(r_k,\phi_k) = \Re_\theta^{-1}\{\hat{g}_w(r_k,\theta_k)\}$.

   c) A reverse conversion of coordinates is recalculated if necessary: $x_k = r_k\, cos\,\varphi_k$; $y_k = sin\,\varphi_k$.

Thus, each sensor performs two (forward and inverse) Radon transforms. The device of joint processing of signals from N sensors performs inverse Radon transform. When sampling of these transformations' arguments $r_k,\ \varphi_k,\ \rho_k,\ \theta_k$ are replaced by arguments $n_r,\ n_\varphi,\ m_\rho,\ m_\theta$.

In [20] represents the development of application-specific integrated circuit for realization fan-beam fast Radon transform with interpolation on quasi-regular coordinate grids.

5. Conclusions

When searching for through defects in pipelines, to which there is no direct access, it is necessary to use remote sensing methods. The theoretical basis of such methods can be the theory of partial coherence and reconstructive computed tomography based on combined (linear and fan) scanning data.

The principal advantage of image reconstruction by projection for small size or point objects is that a high degree of spatial resolution can be obtained using random acoustic signal (actually, acoustic noise) without necessity coherent processing.

The feasibility of the method and the limits of resolution of the tomographic detection systems rocker-coordinate measuring acoustic noise sources are limited only by the accuracy of synchronization systems, navigation binding capacity data lines and fast processing system calculators.

Tomographic processing algorithm using analyses spatial and temporal spectra (spectra of spatial frequencies) of acoustic noise in a system consisting of several receivers are proposed. Obtained results allows to given the nature of the spectrum in further to modify the traditional algorithms for computer tomography, which will proved radical means to improve the accuracy and resolution of the spatial coordinates of the information system.

6. References

[1] Leak Detection: Technology and Implementation: 2nd edition. By Stuart, Hamilton. Bambos Charalambous Publisher: IWA Publishing, 2020. 200 p.

[2] Ahmad, S.; Ahmad, Z.; Kim, C-H.; Kim, J-M. A Method for Pipeline Leak Detection Based on Acoustic Imaging and Deep Learning. Sensors (Basel). 2022; 22(4):1562. https://doi.org /10.3390/s22041562.

[3] Lin, W.; Wang, F.; Liu, Z.; Wu S.; Qiu X. Pipeline Leak Detection by Using Time-Domain Statistical Features. IEEE Sensors Journal. 2017; 17(19): 6431–6442.

[4] Ting, L; et al. Improvement of acoustic water leak detection based on dual tree complex wavelet transform-correlation method. IOP Conf. Series: Earth and Environmental Science, 2019, 268: 012025.

[5] Tang, X.; Liu, Y.; Zheng, L.; Ma, C.; Wang, H. Leak Detection of Water Pipeline Using Wavelet Transform Method. International Conference on Environmental Science and Information Application Technology. 2009: 217–220. https://doi.org /10.1109/ESIAT.2009.57.

[6] Meinert, D.; Gorny, M.; Pollmann, A.; Chen, J.; Garbi, A. Monitoring Acoustic Noise in Steel Pipelines. Proceedings of the 2008 7th International Pipeline Conference. 2008 7th International Pipeline Conference, Volume 1. Calgary, Alberta, Canada. September 29–October 3, 2008. 509–516. ASME. https://doi.org/10.1115/IPC2008-64115

[7] Krasilnikov, A.I.; Polobyuk, T.A. Installation for physical modeling and experimental investigation of leaks in the pipeline. Metrology and devices. 2014; 1: 147–150.

[8] Hu, Z.; Tariq, S.; Zayed, T. A comprehensive review of acoustic based leak localization method in pressurized pipelines. Mech. Syst. Signal Processing. 2021;161: 107994.

[9] Glentis, G.; Angelopoulos, K. Leakage detection using leak noise correlation techniques: overview and implementation aspects. Proceedings of the 23rd Pan-Hellenic Conference on Informatics, 2019.

[10] Faerman, V.A.; et al. The leak location package for assessment of the timefrequency correlation method for leak location. IOP Conf. Series: Journal of Physics: Conf. Series 803. 2017: 012040.

[11] Krymska A.O. Peculiarities of using computer tomography methods to detect anomalies of long and branched pipelines. International scientific journal "Internauka". 2023; 10. https://doi.org/10.25313/2520-2057-2023-10/

[12] Helgason S. Integral Geometry and Radon Transforms. Springer New York Dordrecht Heidelberg London, 2010. 316 pp.

[13] Herman Gabor T. Image Reconstruction from Projections: Fundamentals of Computerized Tomography. New York: Academic Press, 2010. 297 pp.

[14] Natterer F. The Mathematics of Computerized Tomography / John Wiley & Sons, 1986. 222 pp.

[15] Elouedi I., Fournier R., Nait-Ali A., Hamouda A. The polynomial discrete Radon transform. Signal, Image and Video Processing. 2015; 9 (1): 145 – 154.

[16] Wang M. (Ed.) Industrial Tomography: Systems and Applications. Elsevier Ltd, Cambridge, CB22 3HJ, UK, 2015. 744 pp.
[17] Guiguang Ding, Yuchen Guo, Kai Chen, Chaoqun Chu, Jungong Han, Qionghai Dai. Deep Confidence Network for Robust Image Classification IEEE Trans. Image Proc. 2019; 28 (8): 3752 – 3765.
[18] Ponomarenko O., Bulakovska A. Specifics of Application Fan Radon Transform for Searching Gas Escapes Through Pipelines' Holes. Advanced Computer Systems and Networks: Design and Application. Proc. Of the 6th International Conf. ACSN-2013, Lviv, Ukraine, Sept. 16 – 18, 2013. pp. 165 – 166.
[19] Marple L.S. Digital Spectral Analysis: With Applications (Prentice-Hall Series in Signal Processing) Prentice Hall, Inc., Upper Saddle River, NJ, 1987. 492 p.
[20] Ponomarenko, O., Bulakovskaya, A., Skripnichenko, A. et al. Tomographic application-specific integrated circuits for fast radon transformation. CEUR Workshop Proceedings, 2020; 2654: 339–351.